# Radiotherapy of Liver Metastases

## Comparison of Target Volumes and Dose-Volume Histograms Employing CT- or MRI-Based Treatment Planning

Maciej Pech[1], Konrad Mohnike[1], Gero Wieners[1], Ewa Bialek[1], Oliver Dudeck[1], Max Seidensticker[1], Nils Peters[1, 2], Peter Wust[3], Günther Gademann[2], Jens Ricke[1]

**Purpose:** To assess differences in delineated target volumes of liver metastases using contrast-enhanced CT and different MRI sequences for radiation treatment planning.
**Patients and Methods:** 25 patients with 43 colorectal liver metastases were recruited. Tumor margins were defined by two experienced radiologists. The resulting D90 was assessed and the CT-based 3-D dose distribution merged with the according MRI dataset by employing image fusion. A theoretical D90 as a result of MRI-based treatment planning was assessed for various MRI sequences individually.
**Results:** In venous phase contrast-enhanced CT, the mean tumor volume was 20 ml; T1-weighted (T1w) MRI, 27 ml; contrast-enhanced T1w 42 ml; T2w 65 ml. The difference between the target volumes as assessed by either CT or MRI was 181% for T1w images, 178% for contrast-enhanced T1w, and 246% for T2w sequences. All differences were statistically significant ($p < 0.05$).
The analysis of the dose-volume histograms revealed statistically significant differences (i.e., for the D90) for the different target volumes specified by CT and MRI: mean D90 on CT, 18 Gy; plain T1w, 16 Gy; contrast-enhanced T1w, 15.5 Gy; T2w, 12 Gy. Hence, delineation of a larger target volume in T2w MRI compared to contrast-enhanced CT resulted in a smaller D90.
The mean differences of tumor volumes assessed by CT and plain T1w were significantly higher in the group of patients showing local tumor recurrences as compared to patients with long-term local tumor control ($p = 0.002$).
**Conclusion:** For treatment planning of liver metastases, the use of either plain T1w or T2w sequences is recommended to delineate the clinical target volume as completely as possible and not to miss potential tumor cell congregations in the surroundings as in CT.

**Key Words:** Brachytherapy · Liver metastases · MRI · CT

Strahlenther Onkol 2008;184:256–61
DOI 10.1007/s00066-008-1849-8

**Strahlentherapie von Lebermetastasen. Vergleich von Zielvolumina und Dosis-Volumen-Histogrammen mittels MRT- und CT-gestützter Bestrahlungsplanung**

**Ziel:** Beurteilung von Unterschieden in der Abgrenzung von Zielvolumina bei kontrastmittelverstärkter CT- und MRT-gestützter Bestrahlungsplanung.
**Patienten und Methodik:** 25 Patienten mit 43 Lebermetastasen kolorektalen Ursprungs wurden in dieser Studie untersucht. Zur Definition der Zielvolumina wurden CT- und MRT-Untersuchungen verwendet, die Konturierung der Tumorränder wurde von zwei erfahrenen Radiologen vorgenommen. Die D90 wurde nach Bildfusionierung der CT-basierten dreidimensionalen Dosisverteilungen mit den MRT-Datensätzen beurteilt. Eine theoretische D90 als Resultat der MRT-basierten Bestrahlungsplanung wurde bestimmt.
**Ergebnisse:** In der venösen Phase der kontrastmittelverstärkten CT-Untersuchung betrug das mittlere Tumorvolumen 20 ml; MRT T1-gewichtet (T1w) 27 ml; kontrastmittelverstärkte T1w 42 ml; T2w 65 ml. Die Unterschiede der Zielvolumina im Verhältnis zur CT-gestützten Planung betrugen 181% für T1w-, 178% für kontrastmittelverstärkte T1w- und 246% für T2w-Sequenzen. Alle Unterschiede stellten sich als signifikant heraus ($p < 0,05$). Im Vergleich zur kontrastmittelverstärkten CT resultierte somit das Bemessen des Tumorvolumens im T2w MRT in einer niedrigeren D90.
Die Analyse der Dosis-Volumen-Histogramme zeigte signifikante Unterschiede der verschiedenen Volumina. Die mittlere D90 betrug bei CT 18 Gy, bei nativer T1w 16 Gy, bei kontrastmittelverstärkter T1w 15,5 Gy und bei T2w 12 Gy.
Die mittleren Unterschiede des Zielvolumens durch CT- und native T1w-gestützte MRT-Bestrahlungsplanung waren in der Gruppe der Patienten mit lokalen Tumorrezidiven signifikant höher als in der Gruppe mit langfristiger lokaler Kontrolle ($p = 0,002$).

[1] Department of Radiology and Nuclear Medicine, University of Magdeburg, Germany,
[2] Clinic for Radiation Therapy, University of Magdeburg, Germany,
[3] Department of Radiology, Charité, Campus Virchow Clinic, University of Berlin, Germany.

Received: December 18, 2007; accepted: January 11, 2008

**Schlussfolgerung:** Für die Bestrahlungsplanung der Therapie von Lebermetastasen wird die Verwendung von nativen T1w- oder T2w-Sequenzen zur Abgrenzung des Zielvolumens empfohlen, um eine möglichst vollständige Erfassung der Metastase einschließlich evtl. vorhandener peripherer Tumorausläufer zu erreichen.

**Schlüsselwörter:** Brachytherapie · Lebermetastasen · MRT · CT

## Introduction

Brachytherapy of the liver has been used for palliation of diffuse metastatic disease [4, 11, 19, 25]. Recently, new techniques have been introduced enabling a precise targeting of certain lesions [14, 18]. High-dose single-fraction radiation may be delivered even to multiple intrahepatic targets, since the precision of these techniques spares sufficient amounts of liver parenchyma to prevent liver failure. These methods comprise the percutaneous approach employing stereotactic irradiation as well as the interstitial technique utilizing CT guidance for brachytherapy catheter placement and treatment planning [8, 10, 20].

One critical issue of any radiotherapy is target specification in a set of images [9]. This is specifically true in case of liver metastases, where the contrast between tumor and healthy liver parenchyma is potentially low. Extensive data has been published describing advantages and drawbacks of the use of sonography, CT or MRI for thermal ablation of liver metastases [26, 27, 29]. No clear conclusion has been drawn proving the superiority of any of these techniques, probably because the underlying problem may not only be the actual image quality of a specific method, but also its availability, costs and the complexity of its use. In addition, it remains questionable if microscopic tumor spread beyond the macroscopic tumor border or even a tumor capsule can reliably be depicted with the imaging methods at hand today [16].

To overcome the limitations of image guidance, a safety margin is commonly used to consider the microscopic extension of the cancer disease. In thermal liver metastases ablation, a safety margin of 1 cm has been proposed, if MRI guidance is used [29]. However, the dimension of the safety margin remains intuitive. In light of this problem we assessed the differences of tumor dimensions as depicted by contrast-enhanced CT and different MRI sequences. To evaluate the clinical consequences of the use of CT versus MRI for treatment planning, we used CT-guided brachytherapy as a dosimetric model.

## Patients and Methods

25 patients displaying 43 colorectal liver metastases were included. The patient population comprised 16 men and nine women; the mean age was 64.5 years. The study was approved by the local ethics committee. Written informed consent was obtained from all patients.

Comparison of tumor volumes employed MRI and CT acquired on consecutive days. Spiral CT was performed including iodine contrast media (100 ml Ultravist® 370, flow: 2 ml/s; start delay: 70 s). Image parameters included a slice thickness of 5 mm; increment, 5 mm; table feed, 5 mm.

MRI was performed using a 1.5-T system. The imaging protocol comprised the following sequences: T2-weighted (T2w) UTSE FS (ultra short turbo spin echo fat saturation) (echo time [TE] = 90 ms, repetition time [TR] = 2,100 ms, flip = 90°); T1w GRE (gradient recalled echo) (TE = 5 ms, TR = 30, flip = 30°); T1w GRE (TE = 5 ms, TR = 30 ms, flip = 30°) 20 s post i.v. application of 0.05 mmol/kg Gd-BOPTA.

To assess the tumor volumes as visible on each CT and MRI sequence, tumor margins were defined by two radiologists in consensus using 3-D data-processing software (Amira®, Mercury Computer Systems, Berlin, Germany). The tumor margin was defined as the central tumor plus a potential hyperperfused rim in contrast-enhanced CT and MRI or as hyperintense rim in T2w MRI.

To assess the clinical consequence of treatment planning employing CT versus MRI, we used CT-guided high-dose-rate (HDR) brachytherapy as a model for dosimetric simulation. All patients received CT-guided brachytherapy generating the treatment plan on a contrast-enhanced CT dataset. Details of this technique have been described elsewhere [21]. Following catheter positioning, a 3-D spiral CT was acquired and transferred to the treatment-planning system (Brachy Vision™,Varian, Palo Alto, CA, USA). A $^{192}$Ir source was used to deliver a single-fraction treatment (Gammamed, Varian, Charlottesville, VA, USA).

To simulate the MRI-based target volume and the corresponding D90, the 3-D CT data together with the dose plan acquired with BrachyVision™ were merged with each MRI sequence employing anisoscalar image fusion offered by Amira® [22]. The registration routine of the algorithm has been described by Studholme et al. [28]. Local tumor recurrence was defined as asymmetric tumor growth at follow-up examination or symmetric tumor growth starting with the 6-month follow-up examination. The restriction for symmetric tumor growth as a marker of tumor recurrence only after 6 months was applied to differentiate recurrence from hepatic necrosis in areas of high-dose exposure [21].

For both target volumes and D90s with either contrast-enhanced CT or each MR sequence, a statistical analysis was performed employing the Wilcoxon test.

To assess the potential influence of CT versus MR treatment planning on local tumor control, we compared the target

**Table 1.** Assessment of tumor volumes with venous contrast-enhanced CT and different MRI sequences. p-values indicate the comparison between CT and the according MRI sequence. SD: standard deviation.

**Tabelle 1.** Beurteilung von Tumorvolumina nach Konturierung von kontrastmittelverstärkter CT sowie MRT mit verschiedenen Sequenzen. p-Werte sind für den Vergleich von CT und entsprechenden MRT-Sequenzen angegeben. SD: Standardabweichung.

| Modality | Mean volume (ml) | Minimum (ml) | Maximum (ml) | p-value |
|---|---|---|---|---|
| CT (venous) | 20 (SD 29) | 1 | 128 | Standard of reference |
| T1w | 27.5 (SD 35) | 1 | 125 | < 0.001 |
| T1w + Gd-DTPA | 42 (SD 58) | 1 | 233 | 0.003 |
| T2w | 65 (SD 66) | 6 | 252 | < 0.001 |

**Table 2.** Assessment of the D90 as simulated after dosimetry applying venous contrast-enhanced CT and different MR sequences. p-values indicate the comparison between CT and the according MR sequence.

**Tabelle 2.** Beurteilung der D90 nach Konturierung von kontrastmittelverstärkter CT sowie MRT mit verschiedenen Sequenzen. p-Werte sind für den Vergleich von CT und entsprechenden MRT-Sequenzen angegeben.

| Modality | D90 (Gy) | Minimum (Gy) | Maximum (Gy) | p-value |
|---|---|---|---|---|
| CT (venous) | 18 (SD 6.1) | 4 | 33 | Standard of reference |
| T1w | 16 (SD 6.7) | 2 | 31 | 0.002 |
| T1w + Gd-DTPA | 15.5 (SD 6.9) | 1 | 31 | 0.001 |
| T2w | 12 (SD 5.4) | 3 | 23 | < 0.001 |

volumes as determined in patients with and without local tumor recurrence during follow-up. We employed a Kolmogorov-Smirnov and a Mann-Whitney test.

A p-value < 0.05 was considered statistically significant.

## Results

The mean volume of all tumors based on contrast-enhanced CT was 20 ml (standard deviation [SD] = 29; range: 1–128 ml; median: 10 ml; Table 1). In T2w UTSE FS, the mean tumor volume amounted to 65 ml (SD = 66; range: 6–252 ml, median: 44.5 ml). In T1w GRE images, the mean tumor volume was 27.5 ml (SD = 35; range: 1–125 ml, median: 15 ml). In contrast-enhanced T1w GRE images, the mean tumor volume amounted to 42 ml (SD = 58; range: 1–233 ml median: 22.5 ml; Figure 1).

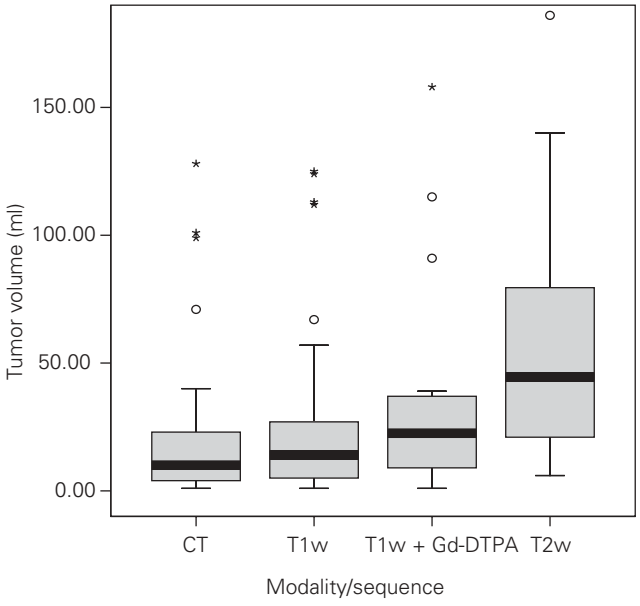


**Figure 1.** Distribution of tumor volumes as visualized with different imaging methods.

**Abbildung 1.** Vergleich von konturiertem Tumorvolumen unter Verwendung verschiedener Bildgebungen.

The differences between CT and MRI dosimetry employing various sequences were significant or highly significant, with MRI showing extensively higher tumor volumes (Table 1). The significance level was also reached comparing T1w GRE and T2w UTSE FS data (p = 0.013), or T2w UTSE FS and contrast-enhanced T1w GRE (p < 0.001).

The mean D90 of all tumors based on contrast-enhanced CT was 18.3 Gy (SD = 6.1; range: 3.9–33 Gy; median: 17 Gy). In T2w UTSE FS, the mean D90 amounted to 12.2 Gy (SD = 5.4; range: 3–23 Gy; median: 10.4 Gy). In T1w GRE images, the mean D90 was 16 Gy (SD = 6.7; range: 2–30.9 Gy; median: 15.4 Gy). In contrast-enhanced T1w GRE images, the mean D90 amounted to 15.5 Gy (SD = 6.9; range: 1–31 Gy; median: 15.5 Gy; Table 2).

Comparing MRI sequences individually, the different outcome of T2w UTSE FS versus nonenhanced T1w GRE was significant (p = 0.014) and for enhanced sequences not significant (p = 0.133).

The median follow-up of all patients was 20 months (SD = 8; range: 1–31 months; median: 17 months). Local tumor control was 81.4%. The difference between target volumes as assessed by either CT or MRI was 181% for T1w images, 178% for contrast enhanced T1w, and 246% for T2w sequences. The differences of tumor volumes assessed by CT and T1w were significantly higher in the group of patients showing local tumor recurrences (Figure 2).

## Discussion

Percutaneous image-guided tumor ablation is depending on the accuracy of the target specification. For such treatment of liver metastases, two basic questions apply: first, does the image modality chosen depict each tumor lesion reliably, and, second, does the imaging modality visualize the true tumor margin? With respect to the first issue, numerous studies have been performed comparing sonography, CT and MRI, the latter including the use of liver-specific contrast agents. Even

though the individual studies often lack statistical power as well as a reliable gold standard, both multislice CT and MRI with liver-specific contrast agents such as iron oxides have been described to reach an accuracy up to 85% for the depiction of liver tumors [3, 12, 30].

In our study, we limited ourselves to variations in the depiction of the tumor margin using different imaging modalities. Due to technical difficulties specifically in the preparation of the specimen, no literature is currently available comparing imaging preferences to histopathology with respect to the exact tumor margin. However, its precise determination will be decisive for local tumor control after treatment, independent of the nature of the technique used for ablation. Unfortunately, an extensive security margin around the radiologically visible tumor is not a perfect solution. Even though small volumes of liver parenchyma have proven remarkable regenerative capacity months after HDR, single-fraction irradiation up to an exposure of 15 Gy [21], specifically repetitive irradiation of different target volumes will endanger liver function, if not enough healthy tissue can be spared. In addition, larger target volumes are associated with higher comorbidity after irradiation [1, 2, 5, 6].

In histopathologic specimens, colorectal metastases of the liver frequently display microscopic tumor spread beyond the macroscopic tumor margin. These microsatellites have been described to predominately originate from blood vessel infiltration or invasion of biliary or lymphatic ducts. The presence of microsatellites as well as the distance to the macroscopic volume correlate with the existence of a pseudocapsule, the extent of the infiltration of lymphocytes around the tumor, and the morphology of the metastases (i.e., nodular vs. oligonodular) [15, 16]. Nanko et al. determined a mean distance of microsatellites to the margin of macrometastases of 7.5 mm ± 8 mm [15]. However, it is very unlikely that, with the radiologic methods at hand, these microdeposits can be depicted, and any safety margin applied should consider their presence. Nevertheless, the question arises which imaging method describes the clinical target volume best.

Differences encountered by applying MRI versus CT reflect the physical preferences of these modalities. In T2w MRI of liver metastases, areas with high proton density such as tumorous tissue will often not be distinguishable from surrounding edema. T1w MRI usually demonstrates a sharply defined tumor margin irrespective of adjacent inflammatory reactions, therefore probably also irrespective of "microscopic" tumor infiltration.

Gd-BOPTA is a hepatocyte-targeted contrast agent. The underlying mechanism for intracellular uptake is a polyspecific organic anionic transport [7, 17]. However, in the first few minutes after i.v. administration the behavior of Gd-BOPTA resembles the standard MRI interstitial contrast agent Gd-DTPA. In our study, we applied the imaging sequence post i.v. application of Gd-BOPTA after 20 s, thus resembling the arterial phase of interstitial contrast agents. Compared to

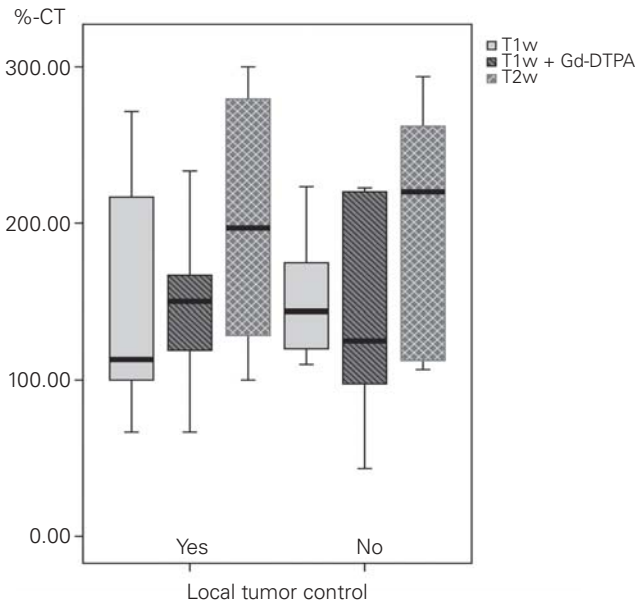


**Figure 2.** Correlation between delineated tumor volume and local tumor control. Tumor volume in CT compared to the according MRI sequence.

**Abbildung 2.** Korrelation von konturiertem Tumorvolumen und lokaler Tumorkontrolle. Vergleich von CT und entsprechender MRT-Sequenz.

nonenhanced T1w sequences, larger tumor volumes as depicted by T2w (i.e., tumor and surrounding edema) or by contrast-enhanced T1w sequences probably reflect the additional inflammatory reaction around the "macroscopic" tumor including microsatellites. We propose that this mechanism will increase the sensitivity for tumor spread of low density beyond the tumor margin, and target delineation should consider edematous or contrast-enhancing tissue at increased risk of carrying tumor cells. However, microscopic tumor spread beyond the radiologically visible tumor involves a significantly reduced tumor cell density (by a factor of 10–100). For this lower cell number a reduced dose will be sufficient for local control.

In our study, we limited the analysis of CT data to an image acquisition during the venous phase, a sequence that is widely used for the detection of liver metastases [13, 23, 24]. During this contrast phase, the contrast agent has shifted from the capillary compartment to the extracellular space. Nevertheless, the actual tumor demarcation proved to be significantly smaller than with MRI including nonenhanced T1w images, a sequence previously described to depict only the gross tumor volume. We assess this result as a surprise, demonstrating the remarkably reduced soft-tissue contrast of even contrast-enhanced CT compared to MRI.

Comparing the group of patients with local tumor control to those displaying tumor recurrence, the variation between CT and MRI assessment was significantly higher in the group

of tumor recurrences (Figure 2). This result was statistically limited to the relative differences between CT and T1w sequences, whereas contrast-enhanced T1w or T2w images missed the statistical threshold. We assess the lack of statistical confirmation for contrast-enhanced T1w and T2w sequences as a consequence of the small patient number included in this study. Nevertheless, a correlation between a higher rate of local recurrences and too small tumor volumes as assessed by CT in comparison to MRI is obvious in our series.

In summary, each MRI sequence depicted larger tumor volumes compared to contrast enhanced CT. Hence, applying MRI instead of CT for treatment planning significantly increases the target volume.

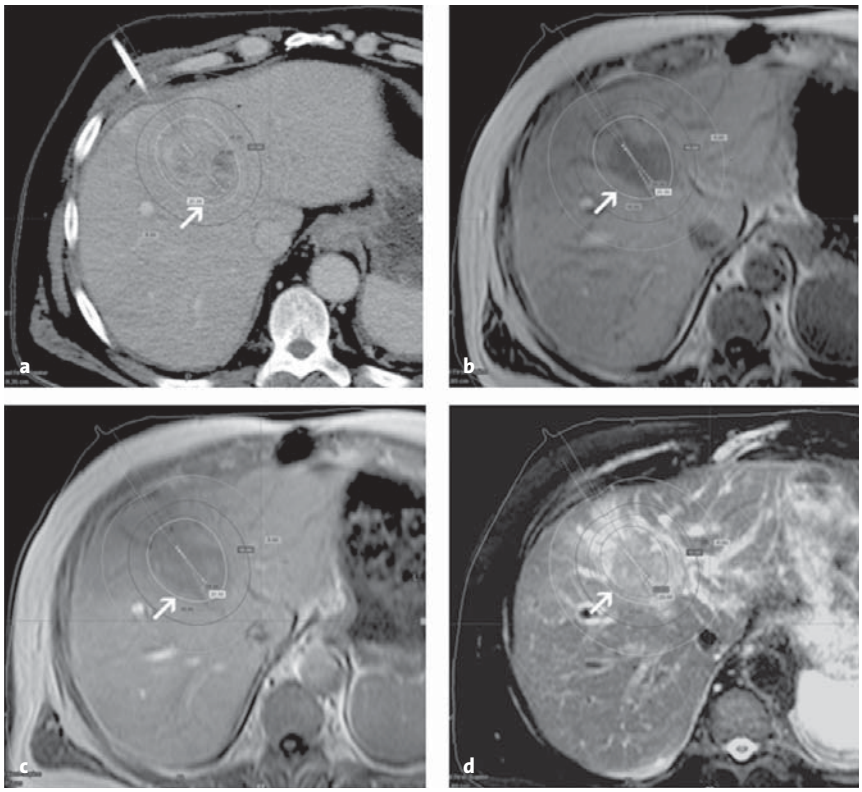


**Figures 3a to 3d.** 59-year-old male with central liver metastasis of a colorectal carcinoma. The arrow marks the 20 Gy isodose line covering the volume of seen metastasis in CT (a). Image fusion with plain T1w (b), T1w with contrast media (c), and T2w (d) MRI sequence. Note the differences in volume demarcation in comparison with the isodose line and the irregular surrounding of the lesion at the 5 o'clock position.

**Abbildungen 3a bis 3d.** 59-jähriger Patient mit zentraler Lebermetastase eines kolorektalen Karzinoms. Der Pfeil markiert die 20-Gy-Isodosenlinie, die das Tumorvolumen in der CT-Untersuchung vollständig umschließt (a). Bildfusion mit nativer T1w- (b), kontrastmittelverstärkter T1w- (c) und T2w-Sequenz (d). Man beachte die Unterschiede in der Volumenabgrenzung insbesondere im Bereich des Außenrandes der Läsion bei 05:00 Uhr.

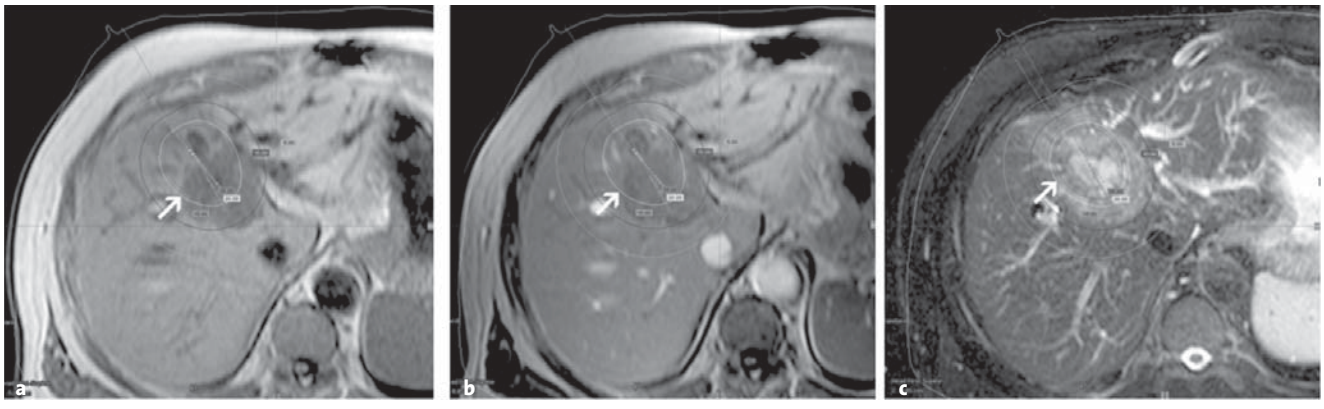


**Figures 4a to 4c.** Same patient with central liver metastasis of colorectal carcinoma after 6 months. The arrow marks the same 20 Gy isodose line. Image fusion with plain T1w (a), T1w with contrast media (b), and T2w (c) MRI sequence shows local growing of the metastasis tissue in same local irregular position at the 5 o'clock position.

**Abbildungen 4a bis 4c.** Derselbe Patient mit zentraler Lebermetastase eines kolorektalen Karzinoms nach 6 Monaten. Der Pfeil markiert die identische 20-Gy-Isodosenlinie. Die Bildfusion mit nativer T1w- (a), kontrastmittelverstärkter T1w- (b) und T2w-Sequenz (c) zeigt lokales Wachstum der Metastase in gleicher Position bei 05:00 Uhr.

## Conclusion

For the treatment planning of liver metastasis, we recommend the use of either plain T1w or T2w MRI images to ensure that the target volume does not only contain "macroscopic" tumor, but also potentially tumor cell-baring inflammatory reaction or microsatellites, respectively (Figures 3 and 4).

## Acknowledgment

This work has been supported by the European Commission Leonardo da Vinci grant.

## References

1. Barendsen GW. Dose fractionation, dose rate and iso-effect relationships for normal tissue responses. Int J Radiat Oncol Biol Phys 1982;8:1981–97.
2. Barendsen GW, Van Bree C, Franken NA. Importance of cell proliferative state and potentially lethal damage repair on radiation effectiveness: implications for combined tumor treatments [Review]. Int J Oncol 2001;19: 247–56.
3. Bluemke DA, Paulson EK, Choti MA, et al. Detection of hepatic lesions in candidates for surgery: comparison of ferumoxides-enhanced MR imaging and dual-phase helical CT. AJR Am J Roentgenol 2000;175:1653–8.
4. Borgelt BB, Gelber R, Brady LW, et al. The palliation of hepatic metastases: results of the Radiation Therapy Oncology Group pilot study. Int J Radiat Oncol Biol Phys 1981;7:587–91.
5. Cheng JC, Wu JK, Huang CM, et al. Radiation-induced liver disease after three-dimensional conformal radiotherapy for patients with hepatocellular carcinoma: dosimetric analysis and implication. Int J Radiat Oncol Biol Phys 2002;54:156–62.
6. Dawson LA, Normolle D, Balter JM, et al. Analysis of radiation-induced liver disease using the Lyman NTCP model. Int J Radiat Oncol Biol Phys 2002;53: 810–21.
7. De Haen C, La Ferla R, Maggioni F. Gadobenate dimeglumine 0.5 M solution for injection (MultiHance) as contrast agent for magnetic resonance imaging of the liver: mechanistic studies in animals. J Comput Assist Tomogr 1999;23:Suppl 1:S169–79.
8. Herfarth KK, Debus J, Lohr F, et al. Stereotactic single-dose radiation therapy of liver tumors: results of a phase I/II trial. J Clin Oncol 2001;19:164–70.
9. Jeanneret-Sozzi W, Moeckli R, Valley JF, et al. The reasons for discrepancies in target volume delineation. A SASRO study on head-and-neck and prostate cancers. Strahlenther Onkol 2006;182:450–7.
10. Kolotas C, Tselis N, Sommerlad M, et al. Reirradiation for recurrent neck metastases of head-and-neck tumors using CT-guided interstitial $^{192}$Ir HDR brachytherapy. Strahlenther Onkol 2007;183:69–75.
11. Leibel SA, Pajak TF, Massullo V, et al. A comparison of misonidazole sensitized radiation therapy to radiation therapy alone for the palliation of hepatic metastases: results of a Radiation Therapy Oncology Group randomized prospective trial. Int J Radiat Oncol Biol Phys 1987;13:1057–64.
12. Lencioni R, Donati F, Cioni D, et al. Detection of colorectal liver metastases: prospective comparison of unenhanced and ferumoxides-enhanced magnetic resonance imaging at 1.5 T, dual-phase spiral CT, and spiral CT during arterial portography. MAGMA 1998;7:76–87.
13. Li L, Wu PH, Mo YX, et al. CT arterial portography and CT hepatic arteriography in detection of micro liver cancer. World J Gastroenterol 1999;5:225–7.
14. Marnitz S, Cordini D, Bendl R, et al. Proton therapy of uveal melanomas: intercomparison of MRI-based and conventional treatment planning. Strahlenther Onkol 2006;182:395–9.
15. Nanko M, Shimada H, Yamaoka H, et al. Micrometastatic colorectal cancer lesions in the liver. Surg Today 1998;28:707–13.
16. Okano K, Yamamoto J, Kosuge T, et al. Fibrous pseudocapsule of metastatic liver tumors from colorectal carcinoma. Clinicopathologic study of 152 first resection cases. Cancer 2000;89:267–75.
17. Pastor CM, Planchamp C, Pochon S, et al. Kinetics of gadobenate dimeglumine in isolated perfused rat liver: MR imaging evaluation. Radiology 2003; 229:119–25.
18. Paulsen F, Scheiderbauer J, Eschmann SM, et al. First experiences of radiation treatment planning with PET/CT. Strahlenther Onkol 2006;182:369–75.
19. Phillips R, Karnofsky DA, Hamilton LD, et al. Roentgen therapy of hepatic metastases. Am J Roentgenol Radium Ther Nucl Med 1954;71:826–34.
20. Ricke J, Seidensticker M, Ludemann L, et al. In vivo assessment of the tolerance dose of small liver volumes after single-fraction HDR irradiation. Int J Radiat Oncol Biol Phys 2005;62:776–84.
21. Ricke J, Wust P, Stohlmann A, et al. CT-guided interstitial brachytherapy of liver malignancies alone or in combination with thermal ablation: phase I–II results of a novel technique. Int J Radiat Oncol Biol Phys 2004;58:1496–505.
22. Rohlfing T, West JB, Beier J, et al. Registration of functional and anatomical MRI: accuracy assessment and application in navigated neurosurgery. Comput Aided Surg 2000;5:414–25.
23. Scott DJ, Guthrie JA, Arnold P, et al. Dual phase helical CT versus portal venous phase CT for the detection of colorectal liver metastases: correlation with intra-operative sonography, surgical and pathological findings. Clin Radiol 2001;56:235–42.
24. Semelka RC, Cance WG, Marcos HB, et al. Liver metastases: comparison of current MR techniques and spiral CT during arterial portography for detection in 20 surgically staged cases. Radiology 1999;213:86–91.
25. Sherman DM, Weichselbaum R, Order SE, et al. Palliation of hepatic metastasis. Cancer 1978;41:2013–7.
26. Solbiati L, Livraghi T, Goldberg SN, et al. Percutaneous radio-frequency ablation of hepatic metastases from colorectal cancer: long-term results in 117 patients. Radiology 2001;221:159–66.
27. Stroszczynski C, Gretschel S, Gaffke G, et al. Laser-induced thermotherapy (LITT) for malignant liver tumours: the role of sonography in catheter placement and observation of the therapeutic procedure. Ultraschall Med 2002;23:163–7.
28. Studholme C, Hill DL, Hawkes DJ. Automated three-dimensional registration of magnetic resonance and positron emission tomography brain images by multiresolution optimization of voxel similarity measures. Med Phys 1997;24:25–35.
29. Vogl TJ, Straub R, Eichler K, et al. Colorectal carcinoma metastases in liver: laser-induced interstitial thermotherapy – local tumor control rate and survival data. Radiology 2004;230:450–8.
30. Ward J, Naik KS, Guthrie JA, et al. Hepatic lesion detection: comparison of MR imaging after the administration of superparamagnetic iron oxide with dual-phase CT by using alternative-free response receiver operating characteristic analysis. Radiology 1999;210:459–66.

**Address for Correspondence**
Maciej Pech, MD
Department of Radiology and Nuclear Medicine
University of Magdeburg
Leipziger Straße 44
39120 Magdeburg
Germany
Phone (+49/391) 671-3030, Fax -3029
e-mail: maciej.pech@med.ovgu.de